Oral Presentation (COSI 2019)

12:30 - 12:45 pm, June 24

Snapshot Incoherent Wavefront Sensing

Congli Wang Qiang Fu Xiong Dun Wolfgang Heidrich

Visual Computing Center, King Abdullah University of Science and Technology (KAUST)

website: congliwang.github.io

email: congli.wang@kaust.edu.sa

Theory: A Model for Classical Wavefront Sensors

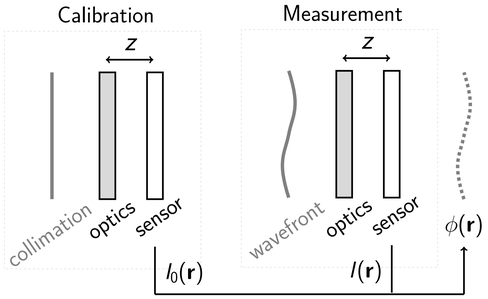

(a) General modeling of wavefront sensors.

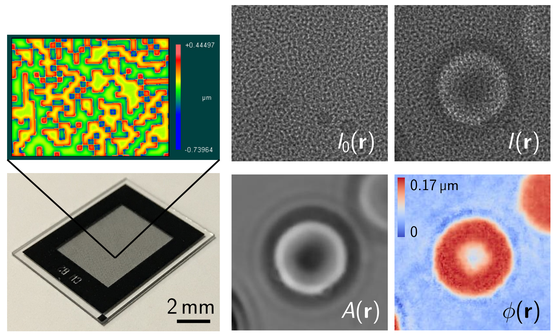

(b) The mask, typical raw images, and the numerical recovery.

Figure 1: (a) The general model. (b) The "optics" for our wavefront sensor (variant of [5]), which recovers amplitude $A(\mathbf{r})$ and phase $\phi(\mathbf{r})$ from reference $I_0(\mathbf{r})$ and measured $I(\mathbf{r})$.

Wavefront sensors are instruments that retrieve phase $\phi(\mathbf{r})$ from wavefront-encoded intensity measurements. For incoherent light, classical wavefront senors are grouped in two categories (probing slopes or curvature):

- Slopes sensors: Shack-Hartmann [1], lateral shearing interferometers [2], coded wavefront sensors [3, 4, 5].
- Curvature sensors: Curvature sensors [6], based on the Transport-of-Intensity Equation (TIE) [7].

Figure 1(a) models wavefront sensors consists of an encoding optics placed distance z away from an intensity sensor, and a numerical algorithm that decodes intensity images ($I_0(\mathbf{r})$ and $I(\mathbf{r})$) to retrieve wavefront $\phi(\mathbf{r})$. At wavelength λ (though it also works for incoherent light), when z is small, we show in either ray or wave optics, that the relationship between $I_0(\mathbf{r})$ and $I(\mathbf{r})$ is:

$$I\left(\mathbf{r}+\frac{\lambda z}{2\pi}\nabla\phi\right) = |A(\mathbf{r})|^2\left(1-\frac{\lambda z}{2\pi}\nabla^2\phi\right) I_0(\mathbf{r}).$$

It is versatile, e.g., TIE can be derived via linearizing $I\left(\mathbf{r}+\frac{\lambda z}{2\pi}\nabla\phi\right)$ around $\mathbf{r}$ at the limit that $z \to 0$. Our model generalizes TIE in: (i) A concise theoretical model for two distanced planes; (ii) Nonlinearity; (iii) More degrees of freedom to allow for a customizable modulation mask (reflected as a user-defined reference image $I_0(\mathbf{r})$).

Table 1: Our equation under different (approximated) forms as commonly seen formulas for each wavefront sensor. $\delta_p(x)$ is the Dirac comb function with period p (the lenslet pitch). $k = 2\pi/\lambda$ is the wave number.

Name	Optics	Commonly seen formula
Shack-Hartmann	micro-lens arrays $I_0(\mathbf{r}) = \delta_p(x)\delta_p(y)$	$I(\mathbf{r}+\frac{\lambda z}{2\pi}\nabla\phi) = I_0(\mathbf{r})$
Lateral shearing	sinusoid gratings (freq. ω) $I_0(\mathbf{r}) = \cos^2(\omega x)\cos^2(\omega y)$	$I(\mathbf{r}) = \lvert A(\mathbf{r})\rvert^2 I_0(\mathbf{r}-\frac{\lambda z}{2\pi}\nabla\phi)$
Curvature sensor	none $I_0(\mathbf{r}) = 1$	$\nabla I_2\cdot\nabla\phi + I_1\nabla^2\phi = \frac{k}{z}(I_1 - I_2) \approx -k\frac{\partial I}{\partial z}$
Coded wavefront sensor	random gratings $I_0(\mathbf{r})$ are speckles	$I(\mathbf{r}+\frac{\lambda z}{2\pi}\nabla\phi) = I_0(\mathbf{r})$ in [5]; or our equation (this work)

Computation: Numerical Solver

The forward model gives N equations but number of unknowns is $2N$ (A and ϕ). For input images $I_0(\mathbf{r})$ and $I(\mathbf{r})$, let $|\tilde{A}|^2 = |A|^2\left(1-\frac{\lambda z}{2\pi}\nabla^2\phi\right)$, we solve the following optimization problem to obtain $\tilde{A}$ and ϕ:

$$\min_{\tilde{A},\phi} \left\| I\left(\mathbf{r}+\frac{\lambda z}{2\pi}\nabla\phi\right) - |\tilde{A}|^2 I_0(\mathbf{r})\right\|_2^2 + \Gamma_{\text{prior}}(\phi, |\tilde{A}|^2),$$

where the prior terms are (parameters $\alpha, \beta, \gamma, \tau$):

$$\Gamma_{\text{prior}}(\phi, |\tilde{A}|^2) = \Gamma_{\text{phase}}(\phi) + \Gamma_{\text{intensity}}(|\tilde{A}|^2),$$

$$\Gamma_{\text{phase}}(\phi) = \alpha\|\nabla\phi\|_1 + \beta\left\|\begin{bmatrix}\nabla\\ \nabla^2\end{bmatrix}\phi\right\|_2^2,$$

$$\Gamma_{\text{intensity}}(|\tilde{A}|^2) = \gamma\left\|\begin{bmatrix}\nabla\\ \nabla^2\end{bmatrix}|\tilde{A}|^2\right\|_1 + \tau\left\|\begin{bmatrix}\nabla\\ \nabla^2\end{bmatrix}|\tilde{A}|^2\right\|_2^2.$$

Using modern optimization the ADMM scheme [8], our solver typically elapses within 100 ms on a Nvidia Titan X (Pascal) GPU for megapixel input images.

Application: Snapshot Incoherent Phase & Intensity Quantitative Phase Microscopy

Our theory reveals a potential to retrieve $|A(\mathbf{r})|^2$ and $\phi(\mathbf{r})$ directly from raw data such as from [5]. As a demonstration, by taking off the condenser lens, we turn an ordinary low-budget bright field microscopy into a simultaneous intensity and phase microscopy, under collimated halogen lamp (HPLS245, Thorlabs) illumination. A prototype coded wavefront sensor is employed which consists of a bare sensor (1501M-USB-TE, Thorlabs) and a random binary phase mask (Fig. 1(b): pixel size 12.9 µm, either 0 or π phase modulation at $\lambda = 550$ nm, placed $z = 1.43$ mm away from the sensor). Figure 2 shows simultaneous amplitude and phase recovery of transparent thin cells. Note how the speckles have been removed and the plausibility of the reconstructed smooth phase maps.

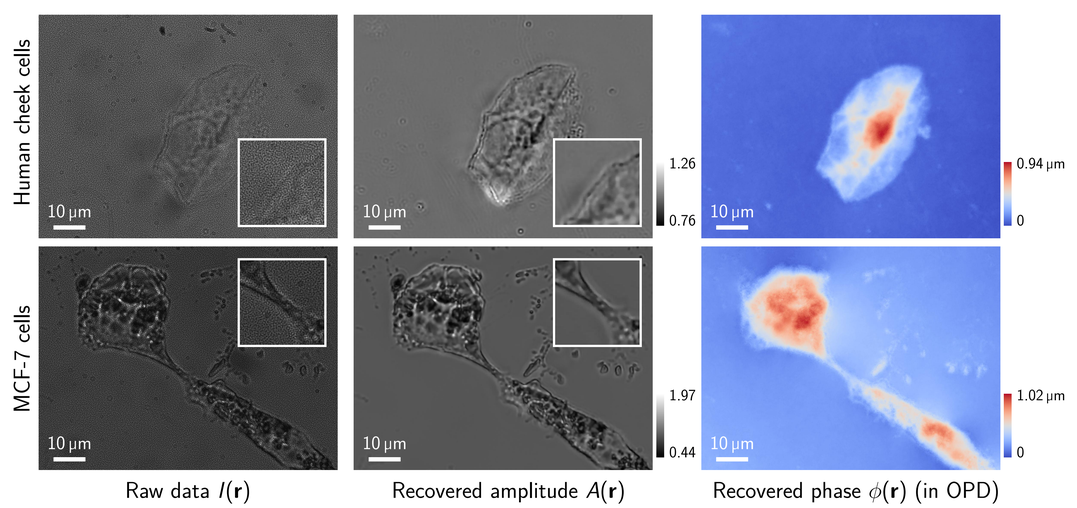

Figure 2: Quantitative phase imaging using our wavefront sensor. Images were taken under an ×100 Mitutoyo plan apochromat objective, 0.70 NA. Inset close-up images show that the speckle patterns have been fully removed from the original raw data.

Acknowledgments & Statement

The authors thank Dr. Fathia Ben Rached, Ioannis Isaioglou, Shahad Alsaiari, and Michael Margineanu for their help in preparing the biological specimens. This work was supported by KAUST Individual Baseline Funding and Center Partnership Funding.

Main paper is under submission to Scientific Reports.

References

[1] R. V. Shack and B. C. Platt, "Production and use of a lenticular Hartmann screen," J. Opt. Soc. Am. A **61**, 656 (1971).

[2] P. Bon, G. Maucort, B. Wattellier, and S. Monneret, "Quadriwave lateral shearing interferometry for quantitative phase microscopy of living cells," Opt. Express **17**, 13080–13094 (2009).

[3] K. S. Morgan, D. M. Paganin, and K. K. Siu, "X-ray phase imaging with a paper analyzer," Appl. Phys. Lett. **100**, 124102 (2012).

[4] S. Bérujon, E. Ziegler, R. Cerbino, and L. Peverini, "Two-dimensional x-ray beam phase sensing," Phys. Rev. Lett. **108**, 158102 (2012).

[5] C. Wang, X. Dun, Q. Fu, and W. Heidrich, "Ultra-high resolution coded wavefront sensor," Opt. Express **25**, 13736–13746 (2017).

[6] F. Roddier, "Curvature sensing and compensation: a new concept in adaptive optics," Appl. Opt. **27**, 1223–1225 (1988).

[7] M. R. Teague, "Deterministic phase retrieval: a green's function solution," J. Opt. Soc. Am. **73**, 1434–1441 (1983).

[8] S. Boyd, N. Parikh, E. Chu, B. Peleato, and J. Eckstein, "Distributed optimization and statistical learning via the alternating direction method of multipliers," Foundations and Trends® in Machine Learning **3**, 1–122 (2011).